International Journal of Science and Technology Research Archive

ISSN: 0799-6632 (Online)

Journal homepage: https://sciresjournals.com/ijstra/

(RESEARCH ARTICLE)

Check for updates

Targeting the M-Ras and B/C-Raf kinases by allosteric druglike inhibitors for cancer therapy

Nicholas A. Nesh *

Department of Physics, office SCP-133 the College of New Jersey 2000 Pennington Road, Ewing, New Jersey, 08628 USA.

International Journal of Science and Technology Research Archive, 2023, 04(01), 143–155

Publication history: Received on 26 December 2022; revised on 05 February 2023; accepted on 07 February 2023

Article DOI: https://doi.org/10.53771/ijstra.2023.4.1.0028

Abstract

Presented here is a computational design of druglike allosteric inhibitors of the M-Ras, B-Raf, and C-Raf kinases. The Ras and Raf kinases are important for cell proliferation. Their mutations can lead to cancer formation. MAPK pathways, important in the cell cycle, are stimulated when Ras activates Raf. Numerous drugs are MAPK inhibitors. Yet, bypass signaling is often established, causing drug resistance. B-Raf inhibitors efficiently inhibit certain MAPK kinases. Nevertheless, they can also activate C-Raf in Ras-mutated cancers, so their signaling is switched from B-Raf to C-Raf. M-Ras can bypass other mutated Ras kinases, leading to cancer advancement. Thus, M-Ras and B/C-Raf are desirable drug targets. Most inhibitors attach to the kinases' catalytic sites. Since these sites are similar in kinases, they are hard to target selectively. Allosteric sites differ in kinases, which allows selective binding. The M-Ras, B-Raf, and C-Raf allosteric binding sites were studied in the Deep View program. New small-molecule inhibitors were designed by systematic atomic substitutions in known inhibitors. The Data Warrior and Molinspiration programs calculated druglike properties of the designed molecules. The molecules with the best druglike properties and no toxicities were docked in ArgusLab. Their binding energies were found. One of the designed molecules bonded well allosterically to B-Raf, C-Raf, and M-Ras and had better druglike properties than the known single-kinase inhibitors. These findings, combined with earlier experimental studies, indicate the molecule designed here may be an effective allosteric inhibitor of all three kinases, and may offer enhanced therapies for cancers with Raf or Ras mutations.

Keywords: Druglike Small Molecules; Allosteric Inhibitors; Kinases; Cancer therapy

1 Introduction

Objective: To computationally design novel druglike small-molecules that could allosterically bind the B-Raf, C-Raf, and M-Ras kinases, in order to prevent the development of drug resistance and potentially stave off cancer progression.

Many cancer patients acquire resistance to chemotherapy treatments [1]. Metastasis develops in as many as 30% to 40% of such patients. The median survival of those patients is about two years [2, 3]. New, more efficient anti-cancer drugs are vitally important for improving the patient outcomes.

Programmed cell death, apoptosis, is a controlled, natural process that eliminates damaged cells [4]. When apoptotic pathways are faulty, damaged cells can survive and become drug insensitive, leading to unrestrained cell growth and cancer propagation [5]. Designing molecules that can circumvent defective apoptotic pathways is crucial for anticancer therapies [6].

Proapoptotic cellular proteins promote cell death, while antiapoptotic ones inhibit it. A damaged cell sends destress signals, which then prompt proapoptotic proteins to deactivate antiapoptotic ones, hence preparing the cell for

* Corresponding author: Nicholas A. Nesh

apoptosis [7]. Normally, this induces a breakdown of the cell's mitochondrial membrane [8], thus initiating cell death. Cancer cells often have damaged apoptotic pathways [9]. Small molecules that interact with regulators of apoptosis can be utilized in cancer treatment [10].

Protein kinases are enzymes involved in numerous cell functions, such as metabolism, transcription immune response, cell division, and apoptosis. As such, kinases are highly regulated [11]. Kinases are important for cancer research due to their prominent roles in many cancers [12, 13]. The activity of a protein can be changed by a kinase via a phosphorylation on its tyrosine, serine, threonine, or histidine residues. This process can either stimulate or inhibit the receptor protein's interactions with other proteins [13].

Small molecules can interact with kinases and either inhibit or activate them [14]. Most kinase inhibitors readily bind to the catalytic site of a kinase [15, 16]. Yet, the catalytic sites of many kinases are very similar in structure to each other, making them challenging to target specifically [17, 18]. The specificity is essential, since drug molecules that can indiscriminately inhibit many kinases may lead to adverse side effects in patients [19].

For some time now, cancer research has focused on designing allosteric kinase inhibitors [20, 21]. Catalytic and allosteric sites of a kinase differ structurally. While the efficacy of catalytic (ATP-competitive) inhibitors significantly varies with the concentration of ATP, an allosteric inhibitor can keep its effectiveness at different ATP concentrations [22, 23]. Given that allosteric sites are dissimilar in different kinases, inhibitors that bind at allosteric sites are less likely to produce adverse side effects. Allosteric druglike inhibitors have been discovered for a comparatively small number of kinases [24, 25].

A MAPK (Mitogen-Activated Protein Kinase) pathway transmits signals from the cell's surface to its nucleus [26]. A mutated protein within a MAPK pathway can become trapped in either its active or inactive state, causing cancer progression [27]. Small molecules that can reverse this can be used for cancer treatments [28].

MAPK kinases are involved in cell proliferation and apoptosis. It turns out that many cancer drugs are MAPK inhibitors (called MAPKi) [27]. Although MAPKi can slow down cancer advancement, bypass pathways are frequently established [29], leading to resistance to MAPKi within a year.

A MAPK pathway is stimulated by a MEK (Mitogen-activated protein kinase) kinase, while MEK kinases are stimulated by Raf kinases [30]. The Raf kinases are A-Raf, B-Raf, and C-Raf. All three are serine/threonine-specific kinases. Given that they influence cellular production and growth, they are well regulated. Downstream, Raf kinases act on MEK1 and MEK2 kinases, which stimulate the extracellular signal-controlled ERK1 and ERK2 kinases [31].

The Raf kinases are activated by Ras G-proteins [31]. Ras are membrane-related proteins. An activated Ras switches on other proteins, ultimately leading to cell survival and division. Damaged Ras signaling has been linked to many cancers. Mutations can generate perpetually activated Ras, which in turn can sustain cell signaling even without inducers. This signaling encourages cell growth and proliferation. Therefore, hyperactive Ras can lead to tumor development [32].

Cancer resistance to treatment is associated with the paradoxical activation of MEK/ERK signaling [33], mostly due to C-Raf stimulation [34, 35]. Mutated Ras does not signal through B-Raf since that leads to excessive ERK signaling, which, in turn, induces apoptosis [36]. Cancer cells with mutated Ras that are resistant to treatment seem to shift their signaling from B-Raf to C-Raf. The reason is that this reduces ERK signaling. Prior research on Ras-mutated cells indicated that B-Raf is not required for ERK activation in such cells [37,38].

Many cancers have mutated Raf kinases, particularly B-Raf, making B-Raf one of the primary targets of cancer drugs [33]. Catalytic-site B-Raf inhibitors efficiently inhibit the kinase in B-Raf-mutant cancer cells. However, they also encourage dimerization of B-Raf with either itself or C-Raf. A mutated upstream activator of Raf can increase C-Raf activation. The creation of a C-Raf-mediated bypass pathways can cause resistance to cancer treatments [31]. Concurrent M-Ras and B/C-Raf inhibition is needed to prevent the development of drug resistance [36].

A drug called Sorafenib can inhibit Raf and several other kinases [39] and it is more selective for C-Raf than for B-Raf [40]. The drug is used to treat some liver, thyroid, and renal cancers [41, 42]. As shown in medical trials, Sorafenib significantly improves disease-free survival, however, it does not increase total survival levels [43]. Additionally, Sorafenib frequently produces troublesome side effects [44].

Vemurafenib is another inhibitor of Raf, which can effectively treat melanomas with certain B-Raf mutations [45]. Yet, as many as 40% of melanomas don't exhibit the mutation and are, consequently, not stopped by the drug. In cases where

Vemurafenib paradoxically promotes the activation of non-mutated B-Raf, it can actually cause cancer advancement [46].

PLX5568 is a medication used against many different tumors that have overactive B-Raf. PLX5568 inhibits cancer progression by blocking faulty regulators of the cell division process [47]. However, PLX5568 interacts with the catalytic site of B-Raf and is, therefore, not specific to the kinase [48]. Previous Medical trials had demonstrated that PLX5568 resistance forms within a few months, causing cancer progression [49].

In cancers with mutated B-Raf, a number of known resistance processes can be overcome by drugs such as PLX7904, PLX7922, and PLX8394 [50]. PLX8394, called a paradox breaker, is a relatively potent inhibitor of Raf. However, only a limited response to this drug was detected in a clinical trial where the cancer shrank by at least 30% in only about 22% of patients [51].

The goals of this work were to computationally design novel small molecules that have better druglike properties than the presently available inhibitors, and could simultaneously inhibit the M-Ras and B/C-Raf kinases at their allosteric sites. That would be particularly valuable in cancers that have mutations of either Ras or B/C-Raf [52].

A small molecule suitable for drug development has to be non-toxic and have bioavailability, metabolic stability, and transport properties similar to those of known drugs. These properties are influenced by the molar mass, polar surface area, electronic bond distributions, hydrophilicity, aqueous solubility, flexibility, and druglikeness of a designed molecule [53, 54].

A druglike molecule should have a relatively low mass, but without sacrificing its effectiveness. Over 80 % of existing drugs have a molar mass below 450 g/mol [55]. Molecules with a higher mass are typically more active than those with a lower mass. However, they are also less likely to reach their intended targets because they are not as readily absorbed.

The absorption of a molecule is significantly affected by its aqueous solubility. Generally, good absorption corresponds to a high value of logS (logarithm of the solubility measured in mol/liter). More than 80% of known drugs have logS greater than - 4, which indicates a solubility of 0.1 mmol/L [55, 56]. For the majority of currently available drugs the logS value is between -4 and 1.

A low logP value (the logarithm of the partition coefficient between n-octanol and water) indicates high hydrophilicity of a molecule [54]. As found in a survey of over 3000 known drugs, the value of logP should be 5 or below for a molecule to be well absorbed [54].

The polar surface area (PSA) is the total surface area of all polar atoms in a molecule. A molecule's PSA value reliably predicts its bioavailability, including its capacity to cross intestinal cell membranes, as well as the blood-brain barrier [56]. Most known drugs have a PSA value of less than 90 $Å^2$ [57]. PSA values greater than this typically indicate lower bioavailability. The oral bioavailability of a molecule is determined by the flexibility of its bonds [58]. The flexibility depends on the number of rotatable bonds in a molecule. Previous studies [59] showed that molecules with fewer than 6 hydrogen bond donors and 10 or fewer rotatable bonds have good oral bioavailability [59].

The main objective of this work was to computationally design novel small molecules with optimal druglike properties that could allosterically bind M-Ras and B/C-Raf kinases, and thus potentially stave off cancer progression.

2 Material and methods

2.1 Computational tools

Putative allosteric inhibitors of M-Ras and B/C-Raf kinases were designed and evaluated using these computational tools: Protein Data Bank [60], ArgusLab [61], Deep View [62], Molinspiration [63], and Osiris DataWarrior [55].

The Protein Data Bank (PDB) [60] is an international database, which contains experimentally found three-dimensional structures of the kinases used in this study, as well as the small molecule inhibitors employed as initial templates. The PDB molecules used in this study were downloaded in the ArgusLab program [61] to investigate their binding sites, perform docking simulations, and determine the properties of bound molecular complexes.

The PDB molecular structures, obtained from the PDB, were visualized in the DeepView program [62]. This program was used to determine atomic distances, charge densities, and H-bonds, as well as to compare the binding sites of several kinases by superimposing them.

The Molinspiration program [63] was employed to study H-bond donors and rotatable bonds, which allowed us to evaluate the drug-like properties of the designed molecules. Potential toxic, mutagenic, tumorigenic, or reproductive risks were analyzed with the DataWarrior program [55], which had been shown to reliably predict these properties [64]. In previous studies, DataWarrior was used to characterize compounds that were known mutagens. The program accurately identified 86% of them as mutagenic. In contrast, it implied only 14% of known drugs from a control group as possible mutagens [55]. Similarly, DataWarrior properly identified as toxic 86% of the examined compounds with known toxicities. However, it flagged as toxic only 8% of the known drugs.

In this work, DataWarrior was used to determine an important molecular property called druglikeness score. A positive value of the score implies a molecule that mostly consists of parts commonly found in known drugs. The methods and validation studies for calculating druglikeness scores are detailed elsewhere [55].

Whether a designed molecule is a good drug candidate cannot be guaranteed by any single molecular property. Nevertheless, an optimal group of druglike atributes, without indicated toxicities or risks, can indicate a molecule that warrants additional experimental studies. The DataWarrior program [55] uses the molar mass, the druglikeness, the logP and logS values, and toxicities to calculate the overall Drug Score of a molecule. The Drug Score is used to evaluate the drug potential of a molecule [55]. The Drug Score values can be between 0 to 1. The greater its value, the more probable that a molecule will be biologically active and non-toxic. As described elsewhere [64], this method effectively differentiates between likely drug candidates and inactive molecules.

2.2 Dataset

The three-dimensional experimental structures of the following complexes were downloaded from the Protein Data Bank [60]: B-Raf bound allosterically to a pyrazolopyridine inhibitor (PDB ID 4G9C) [65], the C-Raf kinase with its allosteric inhibitor (PDB ID 3OMV), and a GDP-bound state of the M-Ras kinase (PDB ID 1X1R).

Fig. 1 a) shows the B-Raf kinase bound allosterically to its known inhibitor pyrazolopyridine [62]. The figure displays the B-Raf residues (yellow balls) that are within a distance of 8 Å from the inhibitor (blue ball and stick). Fig. 1 b) shows a C-Raf allosteric site bound to its ligand. Again, the figure displays only the residues (yellow balls) that are within a distance of 8 Å from the ligand (blue ball and stick). Fig. 1 c) shows the M-Ras allosteric pocket with the residues (yellow balls) within an 8.0 Å radius from its known inhibitor (blue ball-and-stick).

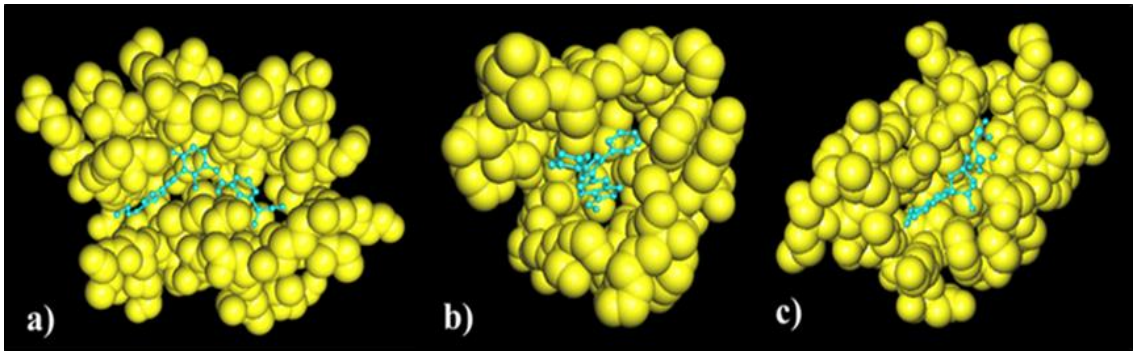

Figure 1 The allosteric pockets of a) B-Raf, b) C-Raf, and c) M-Ras, displaying the kinase residues (yellow balls) within a distance of 8 Å from its known inhibitor (blue ball-and-stick). To enhance visibility, the front-facing kinase residues are not shown

The two-dimensional structures of the known allosteric inhibitors of B-Raf [65], C-Raf [ ], and M-Ras [66] were recreated in Molinspiration and are shown in Fig. 2. As can be seen, the molecules have imidazole groups, benzene rings, and nitrogen atoms. The stability and the binding properties of the molecules are improved by the presence of the cyclic groups. Also, the lack of heavy atoms enhances their biological solubility. The information obtained from analyzing the structures of these inhibitors was used to design new small molecules that could potentially bind all three of the M-Ras and B/C-Raf kinases in their allosteric sites.

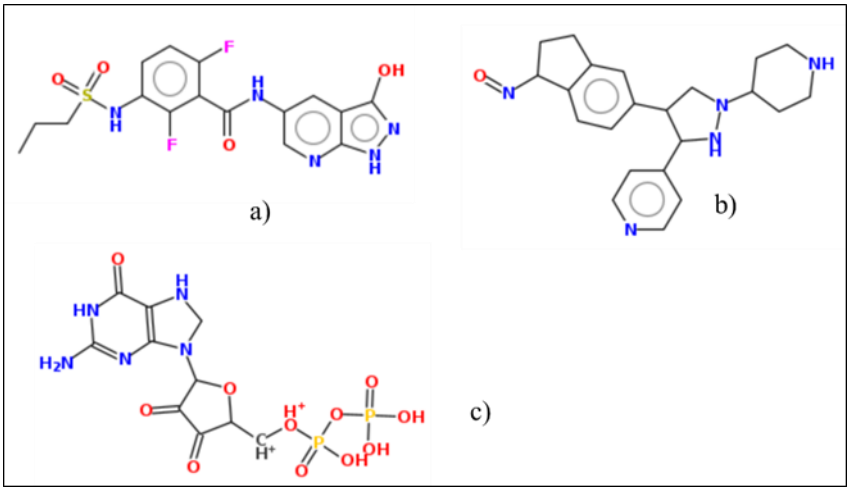

Figure 2 The structures of allosteric inhibitors of a) B-Raf, b) C-Raf, and c) M-Ras

2.3 Procedure employed

The known structures of the M-Ras, B-Raf, and C-Raf kinases' individual inhibitors were uploaded to the DataWarrior program [55] and analyzed. The following properties were studied: molar mass, electronic bond distributions, aqueous solubility, hydrophilicity, flexibility, polar surface area, druglikeness, and toxicities. The net Drug Score was determined. At the end, these properties were assessed by comparing them to those of the newly designed molecules.

The structures of M-Ras, B-Raf, C-Raf with their known inhibitors were uploaded in ArgusLab [61]. Each inhibitor was docked into its respective kinase. The objective was to determine each inhibitor's binding energy in the allosteric site of its kinase and to compare those values to the binding energies of the designed molecules.

The structure of the B-Raf pyrazolopyridine inhibitor was used as an initial template to design novel molecules that could potentially allosterically bind M-Ras, B-Raf, and C-Raf. Over forty molecules were constructed by systematic substitutions of atoms and additions or deletions of ring structures in the known inhibitor. The modifications were chosen so the molecule's druglike characteristics were improved without diminishing its desired properties.

The DataWarrior [55] and Molinspiration [63] programs were employed to find the logP, logS, and PSA values, the number of rotatable bonds, the molar mass, the solubility, the druglikeness, and the number of hydrogen bond donors for each designed molecule. The DataWarrior program also examined any implied toxic and mutagenic risks. The net Drug Score was determined for each molecule. This information was used to systematically design new small molecules with improved druglike properties.

Designed molecules with the best druglike properties and no indicated toxicities or mutagenicities, were then used for the docking studies. The structures of the designed molecules were recreated and optimized in ArgusLab. The Molecule Builder functions and Semiempirical Geometry Optimization [61] were employed. Each of the designed molecules was docked individually into M-Ras, B-Raf, and C-Raf utilizing the ArgusDock function. Rotations of molecular bonds were permitted during the docking. The ascore.prm parameter set, the AScore scoring function, and a 0.4 Å grid resolution were utilized [61]. ArgusLab calculated the binding energies of the stable configurations of each of M-Ras, B-Raf, and C-Raf with the designed molecules. More negative binding energy values meant stronger affinities between the molecule and the kinases. The primary objective was to attain an allosteric binding, while optimizing the molecular overall druglike characteristics.

3 Results and discussion

3.1 Designing putative small molecule inhibitors

DataWarrior [55] and Molinspiration [63] were used to determine the druglike characteristics of the known B-Raf, C-Raf, and M-Ras allosteric inhibitors. The objective was to later compare these properties to those of the designed molecules. The findings are presented in Table 1.

Table 1 Druglike properties of the known B-Raf, C-Raf, and M-Ras inhibitors

Inhibitor of	MM[a)] (g/mol)	logP	logS	PSA (Å^2)	H-donors	Rotatable bonds	Drug Likeness	Drug Score[b)]
B-Raf	411	1.5	-5.7	145	4	6	-0.9	0.22
C-Raf	377	1.1	-2.8	70	2	4	1.4	0.28
M-Ras	441	-11	0.24	249	8	6	-16.3	0.42

a) MM= molar mass b) obtained using a DataWarrior macro routine [68]

As shown in Table 1, the molar masses of all three known inhibitors were in the acceptable range (< 450 g/mol), which suggests good absorptivity [55]. The B-Raf inhibitor had 4 H-bond donors and 6 rotatable bonds, while the C-Raf inhibitor had 2 H-bond donors and 4 rotatable bonds. Both of these sets of numbers were in the preferred range for druglike inhibitors (the number of H-donors < 6 and the number of rotatable bonds < 10). While the M-Ras inhibitor had an acceptable number of rotatable bonds (6), it had 8 H-bond donors [55].

The values of logP were below 5 for all three inhibitors. This suggested that the inhibitors were well absorbed. As indicated by DataWarrior, the B-Raf and M-Ras inhibitors did not have any mutagenic, tumorigenic, irritant, or reproductive risks. However, the C-Raf inhibitor showed elevated mutagenic and tumorigenic risks.

The PSA values of the B-Raf and M-Ras inhibitors were significantly more than 90 Å^2, indicating that the bioavailability of the molecule was probably lower than that of most drugs. The PSA value of the C-Raf inhibitor was lower than 90 Å^2, signifying good bioavailability [55].

For the B-Raf inhibitor, logS < -4. Since -4 is the minimum preferred value, this implies a lower solubility than is usual for known drugs. However, the logS values for the other two inhibitors were in the acceptable range. The overall Drug Score values were 0.22, 0.28, and 0.42 for the B-Raf, C-Raf, and M-Ras inhibitors, respectively. These values were relatively low [55].

Next, we used the structure of the known inhibitors to design molecules with improved druglike characteristics. We performed systematic substitutions of atoms, as well as additions, modifications, and deletions of the cyclic groups in pyrazolopyridine. This allowed us to iteratively create several small molecules that could potentially bind M-Ras and B/C-Raf at their allosteric sites, as well as have improved druglike properties. We designed molecule A that had the best druglike properties and formed the most stable complexes with each kinase. This molecule is shown in Fig. 3.

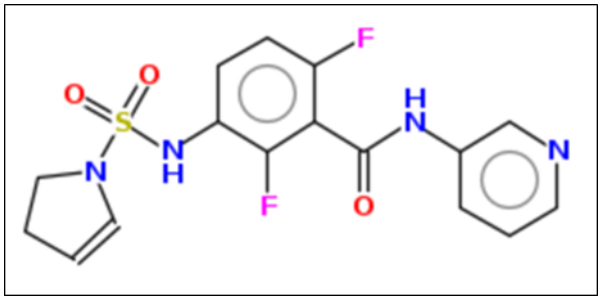

Figure 3 The structure of the designed molecule A that had optimal druglike properties and the highest binding energies with the M-Ras and B/C-Raf kinases

3.2 Evaluation of druglike properties

The druglike properties of the designed molecules were found using Molinspiration [63] and DataWarrior [55]. Fig. 3 shows the designed molecule A that had the best overall druglike characteristics. It also had no implied mutagenic, tumorigenic, irritant, or reproductive risks. The chemical composition of molecule A was $C_{16}H_{17}F_2N_4O_3S$.

DataWarrior and Molinspiration were used to calculate the molar masses (MM), the logP and logS values, the PSA values, and the Drug Likeness. Both programs gave similar values. The number of H-bond donors and rotatable bonds were determined via Molinspiration. The Drug Score was found using a macro routine in DataWarrior [55].

Table 2 summarizes the properties of the designed molecule A as found by Molinspiration and Data Warrior.

Table 2 Druglike properties of the designed molecule A

Molecule	MM[a] (g/mol)	logP	logS	PSA (Å^2)		H-donors	Rotatable bonds	Drug Likeness	Drug Score[b]
A	380	1.3	-4.0	91.4		2	5	2.2	0.74

a) MM= molar mass; b) obtained using a DataWarrior macro routine [68]

The designed molecule A had the logP value of 1.3 (most known drugs have logP < 5.0), Its logS value was -4.0, again in line with the vast majority of commercial drugs, as well as better than the logS value of the B-Raf inhibitor (see Table 1) [55].

The designed molecule A had the polar surface area (PSA) of 91.4 Å^2, indicating good bioavailability. This value is comparable to a value of about 90 Å^2 for known drugs and lower than that of the existing B-Raf and M-Ras inhibitors. The molar mass of molecule A was 380 g/mol, which is comparable to the molar masses of over 80 % of known drugs. Also, the molar mass value was smaller than the values of the known M-Ras and B-Raf kinase inhibitors, indicating better absorptivity.

The numbers of H-bond donors and rotatable bonds were indicative of good oral bioavailability. The druglikeness value of the designed molecule A was 2.2, which was much better than the druglikeness values of the known B-Raf, C-Raf, and M-Ras inhibitors. As discussed earlier, these values dependably indicate the overall drug potential of the designed molecule [55, 56, 61].

Molecule A had the Drug Score value of 0.74, which was about three times larger than the values for the inhibitors of B-Raf and C-Raf, and almost two times larger than the value for the M-Ras inhibitor. As mentioned in the Introduction section, Drug Score values can range from 0 to 1 and predict the molecules' overall drug potential [55]. The closer to 1 the Score is, the likelier the molecule is to be biologically active and non-toxic [63].

3.3 Allosteric binding of designed molecules

To establish the reference values, the known allosteric inhibitors were docked in the M-Ras, B-Raf, and C-Raf kinases in the ArgusLab program [61]. The properties of allosteric binding sites of B-Raf, C-Raf, and M-Ras, were evaluated. Table 3 shows that the binding energy of the respective inhibitors were -36.8 kJ/mol with B-Raf, -39.3 kJ/mol with C-Raf, and -23.3 kJ/mol with M-Ras. The more negative the binding energy, the higher the affinity and the stronger the bond between the small molecule and the kinase [61].

ArgusLab was next used to dock the designed molecule A to M-Ras, B-Raf, and C-Raf. Table 3 shows the binding energies of the resulting complexes. The most stable complex of molecule A was with C-Raf, binding it allosterically with an energy of -39.8 kJ/mol. Molecule A bonded B-Raf and M-Ras with binding energies of -37.1 kJ/mol and -26.9 kJ/mol, respectively. These values were somewhat higher than those for the known inhibitors, indicated a good affinity of the designed molecule A toward all these kinases [61].

Table 3 The binding energies of B-Raf, C-Raf, and M-Ras and the designed Molecule A compared to the binding energies of the kinases with their known inhibitors

Designed Molecule	B-Raf (kJ/mol)	C-Raf (kJ/mol)	M-Ras (kJ/mol)
known inhibitor	-36.8	-39.3	-23.3
A	-37.1	-39.8	-26.9

Therefore, molecule A could bond allosterically to all three kinases with a comparable affinity and much improved drug-like properties when compared to the known inhibitors [60]. In Fig. 4, we show molecule A (green ball-and-stick) in the B-Raf allosteric pocket (gray balls). For comparison, the pyrazolopyridine inhibitor (pink ball-and-stick) bonded to the B-Raf allosteric pocket is also shown.

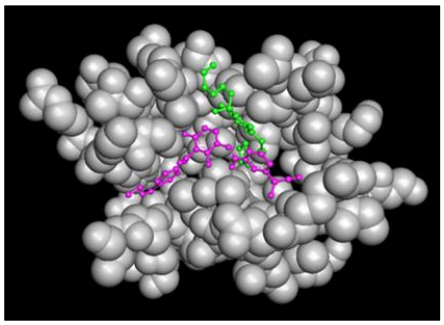

Figure 4 The designed molecule A (green ball-and-stick) is shown bound in the B-Raf allosteric site of (gray balls). For comparison, the pyrazolopyridine inhibitor (pink ball-and-stick) is also shown inside the B-Raf allosteric pocket. To enhance visibility, the front-facing B-Raf residues are removed

The B-Raf residues within a 3.5-Å radius from molecule A, as found in ArgusLab, were: Glu-501, Leu-505, Leu-514, Ile-527, and Thr-529 (Fig. 5). Three of these residues were non-polar (Leu-505, Leu-514, Ile-527). They interact through hydrophobic and van der Waals forces and likely stabilized the binding of molecule A in the allosteric pocket [69].

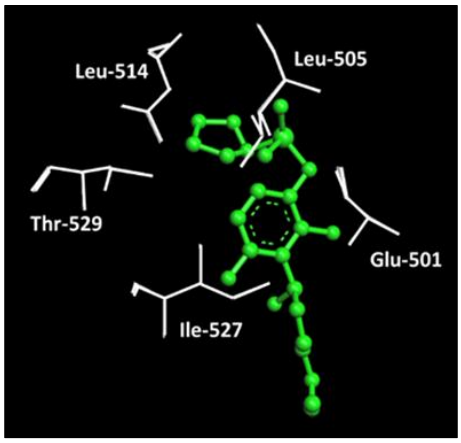

Figure 5 B-Raf residues (wireframe) within a distance of 3.5 Å from molecule A (green ball-and-stick). The orientation of the molecules is such as to optimize their visibility

Molecule A (green ball-and-stick in Fig. 6) was then docked in the allosteric pocket of C-Raf (gray balls). The known inhibitor (pink ball-and-stick) is superimposed in the allosteric pocket of C-Raf to allow a better comparison.

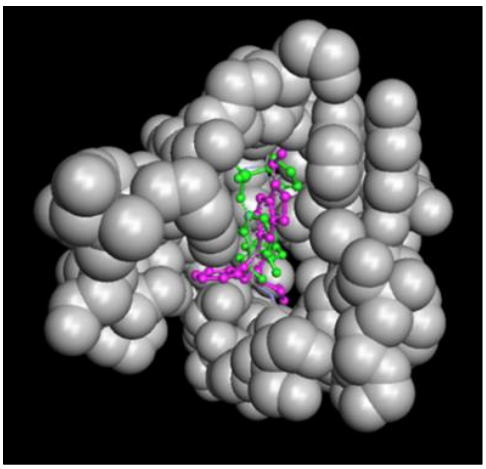

Figure 6 The designed molecule A (green ball-and-stick) is bound in the allosteric site of C-Raf (gray balls). For comparison, the known C-Raf inhibitor (pink ball-and-stick) is also shown in the allosteric site. For clarity, the front-facing C-Raf residues are not shown

Fig. 7 shows the C-Raf residues found within a distance of of 3.5 Å from molecule A (green ball-and-stick): Val 363, Ala 373, Leu 406, Trp 423, Cys 424, Gly 426, Ser 427, and Phe 475. The residues Val 363, Ala 373, Leu 406, Trp 423, and Phe 475 are non-polar residues and likely stabilize the ligand via hydrophobic and van der Waals interactions [69].

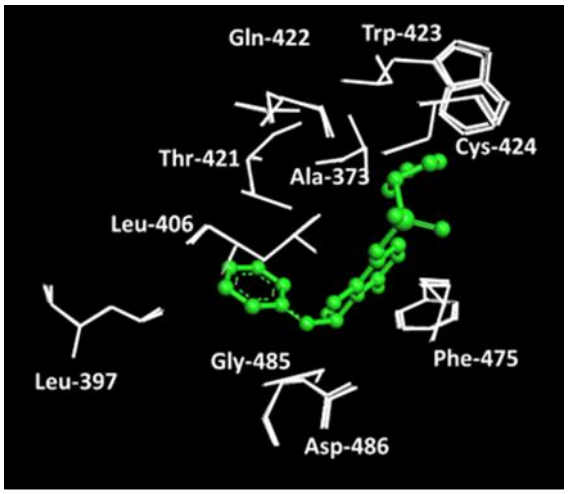

Figure 7 C-Raf residues (wireframe) within a distance of 3.5 Å from molecule A (green ball-and-stick). The orientation of the molecules is such as to optimize their visibility

Molecule A (green ball-and-stick in Fig. 8) was next docked in the allosteric pocket of M-Ras (gray balls). For reference, the known M-Ras inhibitor (pink ball-and-stick) is superimposed in the allosteric pocket of M-Ras.

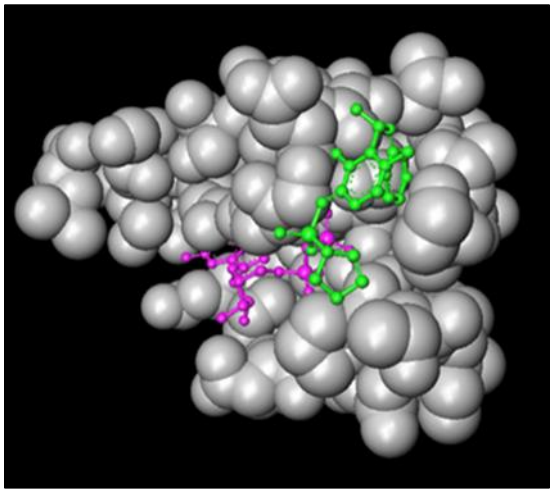

Figure 8 The designed molecule A (green ball-and-stick) is bound in the allosteric site of M-Ras (gray balls). For comparison, the known M-Ras inhibitor (pink ball-and-stick) is also shown bound to the M-Ras allosteric pocket. For clarity, the front-facing C-Raf residues are not shown

Fig. 9 shows the residues of M-Ras found within a distance of 3.5 Å from molecule A (green ball-and-stick): Gly-20, Asp-21, Gly-22, Lys-26, Pro-44, Thr-45, Thr-68, Ala-69, and Gly-70. Four of these residues, Gly-20, Gly-22, Pro-44, and Ala-69 are non-polar. They likely stabilize the binding of molecule A inside the allosteric pocket through van der Waals and hydrophobic interactions.

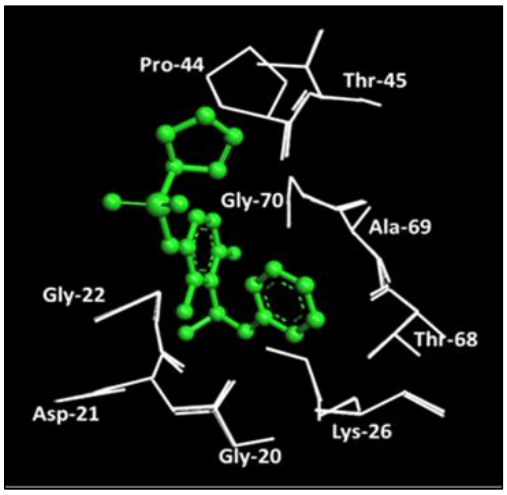

Figure 9 M-Ras residues (wireframe) within a distance of 3.5 Å from molecule A (green ball-and-stick). The orientation of the molecules is such as to optimize their visibility

4 Conclusion

We designed and studied novel small molecule inhibitors that could potentially bind M-Ras and B/C-Raf kinases allosterically. Designed molecule A with optimal druglike properties and no indicated toxicities warrants further studies. Its molar mass was 380 g/mol, which compares favorably to the molar masses of the known drugs. The molecule also had the logP value of 1.3 (which is significantly lower than an acceptable value of 5), 2 H-bond donors and 5 rotatable bonds. The logS and PSA values of the designed molecule favorably compared to those of the known inhibitors. The designed molecule A had a positive druglikeness value and showed no mutagenic, toxic, or reproductive risks. The Drug Score of molecule A was several times greater than for the known inhibitors. All these properties dependably predict the overall drug potential of molecule A and indicate its good biological activity, as described in the Introduction section.

Molecule A made stable complexes with B-Raf, C-Raf, and M-Ras, binding each of them at their allosteric sites, with binding energies of -37.1 kJ/mol, -39.8 kJ/mol, and -26.9 kJ/mol, respectively. These values compare well to those of the known inhibitors, indicating similar affinities to the kinases.

The designed molecule A formed stable complexes with M-Ras and B/C-Raf kinases in computational studies. Its efficacy as a cancer drug eventually needs to be evaluated in vitro and, if justified, in vivo. Molecule A was designed using a known inhibitor as a template. The molecule bonded allosterically to the same binding pockets as the known kinase inhibitors. Moreover, its druglike properties were similar to or better than those of the known inhibitors.

These findings, together with previous experimental research on known inhibitors, imply that the molecule designed here may be very suitable for simultaneous inhibition of M-Ras and B/C-Raf at their allosteric sites. The simultaneous inhibition would cause fewer side effects and would potentially avoid the occurrence of drug resistance in cancers with Ras or B/C-Raf mutations.

Compliance with ethical standards

Disclosure of conflict of interest

The author declare that the research was conducted in the absence of any commercial or financial relationships that could be construed as a potential conflict of interest.

References

[1] Mansoori B, Mohammadi A, Davudian S, Shirjang S, Baradaran B. The Different Mechanisms of Cancer Drug Resistance: A Brief Review. Adv Pharm Bull. 2017 Sep;7(3):339-348. doi: 10.15171/apb.2017.041. Epub 2017 Sep 25. PMID: 29071215; PMCID: PMC5651054.

[2] Siegel RL, Miller KD, Jemal A. Cancer statistics, 2018. CA Cancer J Clin. (2018) 68:7–30. doi: 10.3322/caac.21442

[3] Noone AM, Howlader N, Krapcho M, Miller D, Brest A, Yu M, et al. SEER Cancer Statistics Review, 1975-2015. Bethesda, MD: National Cancer Institute. Available online at: https://seer.cancer.gov/ (2018).

[4] Vaux DL, Cory S, Adams JM. Bcl-2 gene promotes haemopoietic cell survival and cooperates with c-myc to immortalize pre-B cells. Nature 1988; 33, 440.

[5] Campos L, Rouault JP, Sabido O. High expression of bcl-2 protein in acute myeloid leukemia cells is associated with poor response to chemotherapy. Blood 1993; 81, 3091.

[6] Pistritto G, Trisciuoglio D, Ceci C, Garufi A, D'Orazi G. Apoptosis as anticancer mechanism: function and dysfunction of its modulators and targeted therapeutic strategies. Aging (Albany NY). 2016 Apr;8(4):603-19. doi: 10.18632/aging.100934. PMID: 27019364; PMCID: PMC4925817.

[7] Letai A, Bassik MC, Walensky LD, et al. Distinct BH3 domains either sensitize or activate mitochondrial apoptosis, serving as prototype cancer therapeutics. Cancer Cell 2002; 2, 183.

[8] Chipuk JE, Kuwana T, Bouchier-Hayes L. Direct activation of Bax by p53 mediates mitochondrial membrane permeabilization and apoptosis. Science 2004; 303(5660):1010.

[9] Lowery DM, Lim D, Yaffe MB. Structure and function of Polo-like kinases. Oncogene 2005; 24:248.

[10] Carneiro BA, El-Deiry WS. Targeting apoptosis in cancer therapy. Nat Rev Clin Oncol. 2020 Jul;17(7):395-417. doi: 10.1038/s41571-020-0341-y. Epub 2020 Mar 23. PMID: 32203277; PMCID: PMC8211386.

[11] Manning G, Whyte DB, Martinez R et al. The protein kinase complement of the human genome. Science 2002; 298 (5600): 1912–34. doi:10.1126/science.1075762

[12] Kothe M, Kohls D, Low S et al. Structure of the Catalytic Domain of Human Polo-like Kinase 1. Biochemistry 2007; 46 (20) 5960–5971.

[13] Cicenas J, Zalyte E, Bairoch A, Gaudet P. Kinases and Cancer. Cancers (Basel). 2018 Mar 1;10(3):63. doi: 10.3390/cancers10030063. PMID: 29494549; PMCID: PMC5876638.

[14] Schmidt D, Scharf MM, Sydow D, Aßmann E, Martí-Solano M, Keul M, Volkamer A, Kolb P. Analyzing Kinase Similarity in Small Molecule and Protein Structural Space to Explore the Limits of Multi-Target Screening. Molecules. 2021 Jan 26; 26(3):629. doi: 10.3390/molecules26030629. PMID: 33530327; PMCID: PMC7865522.

[15] Grover AK. Use of Allosteric Targets in the Discovery of Safer Drugs. Med Princ Pract. 2013 ; 22: 418–426

[16] Huang D, Zhou T, Lafleur K et al. Kinase selectivity potential for inhibitors targeting the ATP binding site: a network analysis. Bioinformatics 2010; 26 (2), 198.

[17] Hanks SK. Genomic analysis of the eukaryotic protein kinase superfamily: a perspective. Genome Biol 2003; 4 (5): 111.

[18] Hanks SK, Hunter T. Protein kinases 6. The eukaryotic protein kinase superfamily: kinase (catalytic) domain structure and classification. FASEB J 1995; 9 (8): 576–596.

[19] Barouch-Bentov R, Sauer K. Mechanisms of drug resistance in kinases. Expert Opin Investig Drugs. 2011 Feb; 20(2):153-208. doi: 10.1517/13543784.2011.546344. PMID: 21235428; PMCID: PMC3095104.

[20] Gagic Z, Ruzic D, Djokovic N, Djikic T, and Nikolic K. Front. Chem., 08 January 2020, Sec. Medicinal and Pharmaceutical Chemistry Volume 7 - 2019 | https://doi.org/10.3389/fchem.2019.00873

[21] Wilhelm A, Lopez-Garcia LA, Busschots K et al. 2-(3-Oxo-1,3-diphenylpropyl)malonic acids as potent allosteric ligands of the PIF pocket of phosphoinositide-dependent kinase-1 development and prodrug concept. J Med Chem 2012; 55: 9817–9830.

[22] Eathiraj S, Palma R, Hirschi M et al. A Novel Mode of Protein Kinase Inhibition Exploiting Hydrophobic Motifs of Autoinhibited Kinases. J Biol Chem. 2011; 286(23): 20677–20687.

[23] Tan X, Osmulski PA, Gaczynska M. Allosteric regulators of the proteasome: potential drugs and a novel approach for drug design. Curr Med Chem 2006; 13: 155–165.

[24] Han B, Salituro FG, Blanco MJ. Impact of Allosteric Modulation in Drug Discovery: Innovation in Emerging Chemical Modalities. ACS Med Chem Lett. 2020 Mar 10;11(10):1810-1819. doi: 10.1021/acsmedchemlett.9b00655. PMID: 33062158; PMCID: PMC7549105.

[25] Amgalan D, Garner TP, Pekson R, et al. A small-molecule allosteric inhibitor of BAX protects against doxorubicin-induced cardiomyopathy. Nat Cancer 2020; 1(3):315-328.

[26] Pongali R, Thammineni P. Cellular and Molecular Diagnostics. In: Advances in Cell and Molecular Diagnostics. 2018: p. 1-32.

[27] Orton RJ, Sturm OE, Vyshemirsky V, et al. Computational modelling of the receptor-tyrosine-kinase-activated MAPK pathway. The Biochemical J. 2005; 392 (Pt 2): 249–61.

[28] Zhong, L., Li, Y., Xiong, L. et al. Small molecules in targeted cancer therapy: advances, challenges, and future perspectives. Sig Transduct Target Ther 6, 201 (2021). https://doi.org/10.1038/s41392-021-00572-w

[29] Wang SJ, Li R, Ng TSC, et al. Efficient blockade of locally reciprocated tumor-macrophage signaling using a TAM-avid nanotherapy". Sci. Advances 2020; 6: 21, 1-18.

[30] Wellbrock C, Karasarides M, Marais R. The Raf proteins take centre stage. Nat Rev Mol Cell Biol. 2004; 5(11): 875-85.

[31] Menzies AM, Long GV, Murali R. Dabrafenib and its potential for the treatment of metastatic melanoma. Drug Des Devel Ther. 2012; 6:391-405.

[32] Brummer T, McInnes C. Raf kinase dimerization: implications for drug discovery and clinical outcomes. Oncogene 2020; 39, 4155–4169.

[33] Haarberg HE, Smalley KS. Resistance to Raf inhibition in cancer. Drug Discov. Today Technol. 2014; 11:27-32.

[34] Hatzivassiliou G, Song K, Yen I. Raf inhibitors prime wild-type Raf to activate the MAPK pathway and enhance growth. Nature Letters 2010; 464(7287):431-435.

[35] Oh YT, Deng J, Yue P, et al. Paradoxical activation of MEK/ERK signaling induced by B-Raf inhibition enhances DR5 expression and DR5 activation-induced apoptosis in Ras-mutant cancer cells. Sci Rep. 2016; 6:26803.

[36] Dumaz N, Hayward R, Martin J, et al. In Melanoma, Ras Mutations Are Accompanied by Switching Signaling from BRaf to CRaf and Disrupted Cyclic AMP Signaling. Cancer Res. 2006; (66) (19) 9483-9491.

[37] Emuss V, Garnett M, Mason C, et al. Mutations of C-Raf are rare in human cancer because C-Raf has a low basal kinase activity compared with B-Raf. Cancer Res. 2005; 65 (21): 9719–26.

[38] Wilhelm SM, Adnane L, Newell P, et al. Preclinical overview of sorafenib, a multikinase inhibitor that targets both Raf and VEGF and PDGF receptor tyrosine kinase signaling. Mol Cancer Ther. 2008; 7 (10): 3129–40.

[39] Keating GM, Santoro A. Sorafenib: a review of its use in advanced hepatocellular carcinoma. Drugs 2009; 69 (2): 223–40.

[40] Smalley KS, Xiao M, Villanueva J, et al. CRaf inhibition induces apoptosis in melanoma cells with non-V600E BRaf mutations. Oncogene. 2009; 28 (1): 85–94.

[41] Nexavar (sorafenib) dosing, indications, interactions, adverse effects, and more. Medscape Reference. WebMD. Cited Feb. 2, 2023.

[42] Nexavar (sorafenib) tablet, film coated [Bayer HealthCare Pharmaceuticals Inc.]. DailyMed. Bayer HealthCare Pharmaceuticals Inc. Nov. 2013. Cited Feb. 2, 2023.

[43] Escudier B, Eisen T, Stadler WM, et al. Sorafenib in advanced clear-cell renal-cell carcinoma. New England Journal of Medicine. 2007; 356 (2): 125–34.

[44] ASCO: Sorafenib Halts Resistant Thyroid Cancer. www.medpagetoday.com. Cited Feb. 2, 2023.

[45] Kortum R.L., Morrison D.K. Path Forward for Raf Therapies: Inhibition of Monomers and Dimers. 2015; 28(3) 279-281.

[46] Chapman PB, Hauschild A, Robert C, et al. Improved survival with vemurafenib in melanoma with BRAF V600E mutation. New Engl J Med 2011; 364: 2507–2516.https://druginfo.nlm.nih.gov/drugportal/name/dabrafenib. Cited Feb. 2, 2023.

[47] https://medlineplus.gov/druginfo/meds/a613038.html. Cited Feb. 2, 2023.

[48] Gibney GT, Zager JS. Clinical development of dabrafenib in BRaf mutant melanoma and other malignancies. Expert Opinion on Drug Metabolism & Toxicol. 2013; 9(7): 893–9.

[49] Flaherty KT, Infante JR, Daud A, et al. Combined BRaf and MEK Inhibition in Melanoma with BRaf V600 Mutations. New England J. Medicine. 2012; 367 (18): 1.

[50] Koumaki K, Kontogianni G, Kosmidou V, et al. BRAF paradox breakers PLX8394, PLX7904 are more effective against BRAFV600E CRC cells compared with the BRAF inhibitor PLX4720 and shown by detailed pathway analysis. Biochim Biophys Acta Mol Basis Dis. 2021; 1867(4):166061.

[51] Janku F. Interim results from a phase 1/2 precision medicine study of PLX8394 – a next generation BRAF inhibitor. 32nd EORTC-NCI-AACR Symposium on Molecular Targets and Cancer Therapeutics, Oct. 2020.

[52] Sommer E, Dry H, Cross D et al. Elevated SGK1 predicts resistance of breast cancer cells to Akt inhibitors. Biochem. J. 2013; 452: 499–508.

[53] Wishart DS, Knox C, Guo AC et al. DrugBank: a knowledgebase for drugs, drug actions and drug targets. Nucleic Acids Res 2008; 36: D901-6.

[54] Law V, Knox C, Djoumbou Y et al. DrugBank 4.0: shedding new light on drug metabolism. Nucleic Acids Res. 2014; 42(1):D1091-7. 24203711. DataWarrior, a Cheminformatics Program for Data Visualization and Analysis http://www.openmolecules.org/datawarrior/. Cited Feb. 2, 2023.

[55] DataWarrior, a Cheminformatics Program for Data Visualization and Analysis http://www.openmolecules.org/datawarrior/. Cited Feb. 2, 2023.

[56] Ertl P, Rohde B, Selzer P. Fast calculation of molecular polar surface area as a sum of fragment-based contributions and its application to the prediction of drug transport properties. J Med Chem 2000; 43: 3714-3717.

[57] Hitchcock SA, Pennington LD. Structure-brain exposure relationships. J Med Chem 2006; 49 (26): 7559–7583. doi:10.1021/jm060642i.

[58] Veber DF, Johnson SR, Cheng H-Y et al. Molecular properties that influence the oral bioavailability of drug candidates. J Med Chem 2002; 45(12): 2615-2623.

[59] Lipinski CA, Lombardo F, Dominy BW et al. Experimental and computational approaches to estimate solubility and permeability in drug discovery and development settings. Adv Drug Delivery Rev 1997; 23: 4-25.

[60] Protein data Bank, http://www.rcsb.org/pdb/home/home.do. Cited Feb. 2, 2023.

[61] Thompson MA, ArgusLab 4.0.1, Planaria Software LLC, Seattle, WA, http://www.arguslab.com/. Cited Feb. 2, 2023.

[62] Guex N and Peitsch MC. SWISS-MODEL and the Swiss-PdbViewer: An Environment for Comparative Protein Modeling. Electrophoresis 1997; 18:2714-2723; http://www.expasy.org/spdbv/. Cited Feb. 2, 2023. http://www.molinspiration.com/. Cited Feb. 2, 2023.

[63] http://www.molinspiration.com/. Cited Feb. 2, 2023.

[64] Richardson C, Williamson D, Parratt M et al. Triazolo[1,5-a]pyrimidines as novel CDK2 inhibitors: protein structure-guided design and SAR. Bioorg Med Chem Lett. 2006; 16(5): 1353-1357.

[65] Pyrazolopyridine inhibitors of B-Raf(V600E). Part 4: Rational design and kinase selectivity profile of cell potent type II inhibitors. Wenglowsky, S., Moreno, D., Laird, E.R., Gloor, S.L., Ren, L., Risom, T., Rudolph, J., Sturgis, H.L., Voegtli, W.C. (2012) Bioorg Med Chem Lett 22: 6237-6241

[66] Hatzivassiliou, G., Song, K., Yen, I., et al. RAF inhibitors prime wild-type RAF to activate the MAPK pathway and enhance growth. (2010) Nature 464: 431-435

[67] Ye, M., Shima, F., Muraoka, S., et al. Crystal Structure of M-Ras Reveals a GTP-bound "Off" State Conformation of Ras Family Small GTPases. (2005) J Biol Chem 280: 31267-31275

[68] Sander T (2015) DataWarrior Macro Calculate Properties.dwam, http://openmolecules.org/forum/index.php?t=msg&th=13&. Cited Feb. 2, 2023.

[69] Roth CM, Neal BL, Lenhoff AM. Van der Waals interactions involving proteins. Biophys J. 1996 Feb;70(2):977-87. doi: 10.1016/S0006-3495(96)79641-8. PMID: 8789115; PMCID: PMC1224998